Nano Nexus & Applications

www.nna.reapress.com

Nano. Nex. App. Vol. 1, No. 2 (2026) 144–160.

Paper Type: Original Article

Nanocellulose/UiO-66-NH_2 Nanocomposite for Efficient Removal of Tetracycline and Ciprofloxacin from Aqueous Solutions

Arezou Baniasad*

Department of Chemical Engineering, Ayatollah Amoli Branch, Islamic Azad University, Amol, Iran; arezou.baniasad@gmail.com.

Citation:

Received: 05 October 2025 *Revised: 03 January 2026* *Accepted: 24 February 2026*	Baniasad, A. (2026). Nanocellulose/UiO-66-NH_2 nanocomposite for efficient removal of tetracycline and ciprofloxacin from aqueous solutions. *Nano Nexus & Applications, 1*(2), 144-160.

Abstract

The increasing occurrence of antibiotic residues in aquatic environments has become a major environmental concern due to their persistence, ecological toxicity, and contribution to the development of antibiotic-resistant bacteria. In the present study, a nanocellulose/UiO-66-NH_2 nanocomposite was synthesized and evaluated as an efficient adsorbent for the removal of tetracycline (TC) and ciprofloxacin (CIP) from aqueous solutions. The physicochemical properties of the synthesized nanocomposite were characterized using Dynamic Light Scattering (DLS), zeta potential analysis, and Brunauer–Emmett–Teller (BET) surface area analysis. The synthesized nanocomposite exhibited an average hydrodynamic particle size of approximately 165 nm, a zeta potential of −31.8 mV, and a BET surface area of approximately 620 m^2/g, indicating good colloidal stability and a well-developed mesoporous structure. Batch adsorption experiments were performed to investigate the effects of solution pH, contact time, and initial antibiotic concentration on adsorption performance. Maximum adsorption efficiency was achieved at pH 7, while adsorption equilibrium was reached within approximately 90 min for both antibiotics. The equilibrium data were better described by the Langmuir isotherm model than by the Freundlich model, indicating predominantly monolayer adsorption. The maximum adsorption capacities obtained from the Langmuir model were 286.4 mg/g for TC and 254.7 mg/g for CIP. The excellent adsorption performance of the synthesized nanocomposite was attributed to the synergistic effects of electrostatic attraction, hydrogen bonding, π–π interactions, pore filling, and coordination interactions between antibiotic molecules and the functional groups of the nanocellulose/UiO-66-NH_2 framework. Furthermore, the adsorbent maintained more than 90% of its initial removal efficiency after five consecutive adsorption–desorption cycles, demonstrating excellent reusability. These findings suggest that the synthesized nanocellulose/UiO-66-NH_2 nanocomposite is a promising, environmentally friendly, and highly efficient adsorbent for the removal of antibiotic contaminants from aqueous environments.

Keywords: Nanocellulose, Nanocomposite, Adsorption, Tetracycline, Ciprofloxacin, Antibiotic removal.

1 | Introduction

The continuous release of pharmaceutical contaminants into aquatic environments has become a major environmental concern over the past two decades [1–3]. Among the various classes of emerging

Corresponding Author: arezou.baniasad@gmail.com

https://doi.org/10.48314/nna.vi.68

contaminants, antibiotics have attracted particular attention because of their extensive consumption in human and veterinary medicine, widespread application in livestock production, and increasing use in aquaculture [4]. Large quantities of antibiotics are continuously discharged into municipal wastewater treatment plants, hospital effluents, pharmaceutical manufacturing wastewaters, and agricultural runoff. Since conventional wastewater treatment systems are not specifically designed to eliminate these biologically active compounds, significant concentrations of antibiotics are continuously released into rivers, lakes, groundwater, and even drinking water resources [4–6]. The persistence of these contaminants in aquatic environments has raised serious environmental and public health concerns because they promote the development and dissemination of antibiotic-resistant bacteria and antibiotic resistance genes, which are now recognized as one of the greatest global health threats [7]. Among the antibiotics frequently detected in aquatic environments, Tetracycline (TC) and Ciprofloxacin (CIP) have received considerable attention owing to their extensive consumption, incomplete metabolism, and high environmental persistence [5–10]. TC is a broad-spectrum antibiotic widely used for the treatment of bacterial infections in both humans and animals. Due to its complex molecular structure and multiple ionizable functional groups, TC exhibits remarkable environmental stability and can strongly interact with dissolved metal ions and natural organic matter. CIP, a second-generation fluoroquinolone antibiotic, possesses excellent antibacterial activity against both Gram-positive and Gram-negative bacteria. However, a substantial fraction of the administered dose is excreted unchanged into wastewater systems, resulting in its frequent detection in municipal wastewater, hospital effluents, surface waters, sediments, and groundwater [11]. Even at trace concentrations, these antibiotics may induce chronic toxicity in aquatic organisms, disrupt microbial ecosystems, and accelerate the spread of antimicrobial resistance. Various treatment technologies have been developed to remove antibiotic contaminants from aqueous environments, including biological degradation, membrane filtration, advanced oxidation processes, photocatalytic degradation, coagulation–flocculation, electrochemical treatment, and adsorption. Although each technique offers specific advantages, many of them suffer from considerable drawbacks such as incomplete pollutant degradation, membrane fouling, sludge generation, high operational costs, excessive energy consumption, or the formation of toxic intermediate products [12]. Among these technologies, adsorption has emerged as one of the most effective and economically attractive methods because of its high removal efficiency, operational simplicity, low energy consumption, ease of operation, and applicability over a wide range of contaminant concentrations [13]. Nevertheless, the overall performance of adsorption processes strongly depends on the physicochemical characteristics of the adsorbent, including its surface area, pore structure, surface functionality, and chemical stability.

Recent advances in nanotechnology have enabled the development of highly efficient nanostructured adsorbents for environmental remediation. Nanomaterials possess exceptionally large specific surface areas, abundant active adsorption sites, tunable pore structures, and high surface reactivity, making them promising candidates for water purification applications. Various nanomaterials, including graphene derivatives, carbon nanotubes, metal oxide nanoparticles, biochar-based nanocomposites, polymeric nanomaterials, and nanocellulose, have demonstrated excellent adsorption performance toward a broad range of organic and inorganic pollutants. However, practical applications of many nano adsorbents remain limited because of nanoparticle aggregation, difficult recovery after treatment, insufficient mechanical stability, and relatively high production costs [10–16].

Nanocellulose has recently emerged as a sustainable and environmentally friendly nanomaterial with significant potential for water purification. Derived from renewable biomass resources, nanocellulose exhibits numerous attractive properties, including biodegradability, low toxicity, excellent mechanical strength, high hydrophilicity, and abundant hydroxyl (-OH) functional groups that enable facile surface modification. Depending on the preparation method, nanocellulose can be classified as Cellulose Nanocrystals (CNC), Cellulose Nanofibrils (CNF), or Bacterial Nanocellulose (BNC). Owing to its high aspect ratio and large specific surface area, nanocellulose can efficiently interact with various contaminants. Moreover, its abundant hydroxyl groups facilitate chemical functionalization and integration with inorganic nanomaterials and porous crystalline structures, thereby significantly improving adsorption performance.

Despite these advantages, pristine nanocellulose generally exhibits limited adsorption capacity toward certain pharmaceutical contaminants because of its relatively low porosity and limited number of active adsorption sites. Consequently, recent studies have focused on combining nanocellulose with highly porous materials to fabricate multifunctional hybrid adsorbents exhibiting synergistic physicochemical properties.

Among advanced porous materials, Metal-Organic Frameworks (MOFs) have attracted tremendous attention because of their exceptionally high specific surface areas, tunable pore structures, adjustable chemical functionalities, and outstanding adsorption capacities. MOFs are crystalline porous materials constructed from metal ions or metal clusters interconnected by organic ligands, forming highly ordered three-dimensional frameworks with abundant accessible adsorption sites [17]. The structural versatility of MOFs enables the rational design of materials with tailored pore sizes and surface chemistries suitable for the selective removal of a wide range of environmental pollutants.

Various MOFs, including UiO-66, UiO-66-NH_2, ZIF-8, MIL-53, and HKUST-1, have demonstrated remarkable adsorption performance toward pharmaceutical contaminants. Among these materials, UiO-66-NH_2, an amino-functionalized zirconium-based MOF, has received considerable attention because of its excellent chemical and thermal stability, remarkable resistance in aqueous environments, and the presence of amino groups that provide additional active sites for adsorption. The amino-functionalized surface enhances the interaction between the adsorbent and antibiotic molecules through hydrogen bonding, electrostatic attraction, π–π interactions, and coordination interactions, making UiO-66-NH_2 a highly promising adsorbent for water purification applications [17–20]. Despite these advantages, the practical application of pristine UiO-66-NH_2 remains restricted by several limitations, including particle aggregation, relatively poor mechanical properties, and difficulties associated with material handling and recovery after adsorption. To overcome these drawbacks, integrating UiO-66-NH_2 with renewable biopolymers such as nanocellulose has emerged as an effective strategy for developing advanced hybrid adsorbents [11].

In the nanocellulose/UiO-66-NH_2 nanocomposite, the nanocellulose matrix acts as a biodegradable and mechanically robust supporting framework that promotes the uniform dispersion of UiO-66-NH_2 nanoparticles, suppresses particle aggregation, improves structural stability, and enhances the accessibility of adsorption sites. Simultaneously, UiO-66-NH_2 contributes a highly porous crystalline network with abundant active sites and large surface area, substantially improving the adsorption capacity of the hybrid material. The synergistic combination of nanocellulose and UiO-66-NH_2 therefore offers several advantages, including enhanced adsorption efficiency, improved structural stability, excellent environmental compatibility, and easier handling during water treatment processes [10].

Although numerous studies have investigated MOF-based adsorbents for the removal of pharmaceutical contaminants, relatively few have focused on nanocellulose/UiO-66-NH_2 nanocomposites for the simultaneous adsorption of TC and CIP under different operational conditions. Furthermore, a comprehensive understanding of the relationships between the physicochemical properties of the nanocomposite and its adsorption behavior remains limited. Investigating the effects of solution pH, contact time, adsorbent dosage, and initial antibiotic concentration, together with adsorption equilibrium and regeneration performance, is essential for evaluating the practical applicability of this class of sustainable bio-based adsorbents in wastewater treatment [11–13].

The present study aimed to synthesize a nanocellulose/UiO-66-NH_2 nanocomposite as an environmentally friendly and highly efficient adsorbent for the removal of TC and CIP from aqueous solutions. The synthesized nanocomposite was characterized using Dynamic Light Scattering (DLS), zeta potential analysis, and Brunauer–Emmett–Teller (BET) surface area analysis to evaluate its particle size distribution, colloidal stability, and porous characteristics. Batch adsorption experiments were carried out to investigate the effects of solution pH, adsorbent dosage, contact time, and initial antibiotic concentration on adsorption performance. In addition, adsorption equilibrium was evaluated using the Langmuir and Freundlich isotherm models, while the adsorption mechanism and regeneration performance of the synthesized nanocomposite

were systematically investigated. The findings of this study provide valuable insights into the development of sustainable bio-based MOF nanocomposites for the efficient removal of antibiotic contaminants from aqueous environments.

2 | Materials and Methods

2.1 | Materials

Nanocellulose was used as the supporting biopolymer for the preparation of the nanocomposite adsorbent. All chemicals employed in this study were of analytical grade and were used without further purification. Zirconium chloride ($ZrCl_4$) and 2-aminoterephthalic acid (NH_2-BDC), used as the metal precursor and organic linker for the synthesis of UiO-66-NH_2, were purchased from commercial suppliers. TC hydrochloride and CIP hydrochloride were selected as model antibiotic contaminants. Sodium hydroxide (NaOH) and hydrochloric acid (HCl) were used for pH adjustment throughout the adsorption experiments. Deionized water was used in all synthesis procedures and adsorption studies.

2.2 | Preparation of the Nanocellulose/UiO-66-NH_2 Nanocomposite

The nanocellulose/UiO-66-NH_2 nanocomposite was synthesized via an in-situ growth method. Initially, nanocellulose was dispersed in deionized water under magnetic stirring followed by ultrasonic treatment to obtain a homogeneous suspension. Separately, $ZrCl_4$ and 2-aminoterephthalic acid were dissolved in the appropriate solvent under continuous stirring. The nanocellulose suspension was gradually introduced into the precursor solution, allowing the nucleation and growth of UiO-66-NH_2 crystals on the nanocellulose surface. The reaction mixture was maintained under controlled temperature and continuous stirring to ensure complete crystallization of the MOF. After synthesis, the obtained nanocomposite was separated by centrifugation, repeatedly washed with deionized water and ethanol to remove residual reactants, and dried at an appropriate temperature until a constant weight was obtained. The dried nanocomposite was stored in airtight containers for subsequent characterization and adsorption experiments [19].

2.3 | Characterization of the Nanocomposite

The hydrodynamic particle size distribution and Polydispersity Index (PDI) of the synthesized nanocellulose/UiO-66-NH_2 nanocomposite were determined using DLS. Prior to measurement, the samples were ultrasonically dispersed in deionized water to obtain a homogeneous suspension. The surface charge and colloidal stability of the synthesized nanocomposite were evaluated using zeta potential analysis at room temperature. The specific surface area, total pore volume, and average pore diameter of the synthesized nanocomposite were determined using nitrogen adsorption–desorption analysis based on the BET method. Before analysis, the samples were degassed under vacuum to remove physically adsorbed moisture and gases [17–19]

2.4 | Batch Adsorption Experiments

Batch adsorption experiments were carried out to evaluate the adsorption performance of the synthesized nanocellulose/UiO-66-NH_2 nanocomposite toward TC and CIP. A predetermined amount of adsorbent was added to antibiotic solutions of known concentration in sealed Erlenmeyer flasks. The suspensions were agitated using a thermostatically controlled orbital shaker at a constant shaking speed. The influence of operational parameters, including solution pH, contact time, adsorbent dosage, and initial antibiotic concentration, on the adsorption performance was systematically investigated. After adsorption equilibrium was reached, the suspensions were centrifuged, and the residual antibiotic concentration in the supernatant was determined using UV-Visible spectrophotometry [20–22]. The adsorption capacity (q, mg/g) and removal efficiency (R, %) were calculated according to the following *Eqs. (1)* and *(2)*:

$$R(\%) = \frac{Co - Ce}{Co} \times 100, \quad (1)$$

$$qe = \frac{m(Co - Ce)V}{m}, \quad (2)$$

where C_0 and C_e (mg/L) are the initial and equilibrium antibiotic concentrations, respectively, V (L) is the solution volume, and m (g) is the mass of the adsorbent.

2.5 | Adsorption Isotherm Analysis

The equilibrium adsorption data were analyzed using the Langmuir and Freundlich isotherm models to evaluate the adsorption behavior of TC and CIP onto the synthesized nanocomposite. The corresponding isotherm parameters were obtained by fitting the experimental equilibrium data to the linearized forms of the two models. The goodness of fit was evaluated using the correlation coefficient (R^2) [17].

2.6 | Regeneration and Reusability

The regeneration performance of the synthesized nanocomposite was evaluated through consecutive adsorption desorption cycles. After each adsorption experiment, the spent adsorbent was regenerated using an appropriate desorbing solution, washed thoroughly with deionized water, dried, and reused in subsequent adsorption cycles. The adsorption efficiency after each cycle was recorded to assess the stability and reusability of the prepared nanocomposite [19], [20].

3 | Results and Discussion

3.1 | Dynamic Light Scattering Analysis

DLS analysis was performed to investigate the hydrodynamic particle size distribution and dispersion stability of the synthesized nanocomposite. The DLS results indicated that the prepared nanocomposite exhibited a nanoscale hydrodynamic diameter of approximately 165 nm with a PDI value of 0.24, suggesting a relatively uniform particle size distribution and good dispersion stability in aqueous media. The nanoscale particle size confirms the successful formation of a hybrid nanostructure consisting of UiO-66-NH_2 nanoparticles integrated within the nanocellulose framework. The presence of nanocellulose provides a suitable supporting matrix for controlling UiO-66-NH_2 crystal growth and limiting excessive aggregation of UiO-66-NH_2 particles through steric stabilization and surface interactions. This behavior leads to improved dispersion of the active components and enhances the accessibility of adsorption sites. The obtained PDI value indicates a relatively homogeneous distribution of nanocomposite particles. A narrow particle size distribution is highly desirable for adsorption applications because uniformly dispersed nanoparticles provide a larger accessible surface area and facilitate the diffusion of antibiotic molecules into the porous structure of the UiO-66-NH_2 component. The nanoscale characteristics of the synthesized nanocomposite are expected to improve the adsorption performance toward TC and CIP by reducing diffusion limitations and increasing the interaction between contaminant molecules and available active sites. *Table 1* summarizes the typical particle size characteristics and dispersion behavior of MOF-based nanocomposite systems.

Table 1. DLS characteristics of MOF-based nanocomposite systems.

Material/System	Hydrodynamic Particle Size (nm)	PDI Range	Interpretation
Pristine UiO-66-NH_2 nanoparticles	50-200	0.15-0.40	Formation of nanosized UiO-66-NH_2 particles with possible aggregation depending on synthesis conditions.
Nanocellulose-supported UiO-66-NH_2 composite	80-300	0.20-0.40	Improved dispersion and reduced aggregation due to the nanocellulose supporting matrix.
Nanocellulose/UiO-66-NH_2 nanocomposite hybrid adsorbent	100-250	<0.30	Favorable nanoscale distribution and improved accessibility of adsorption sites.

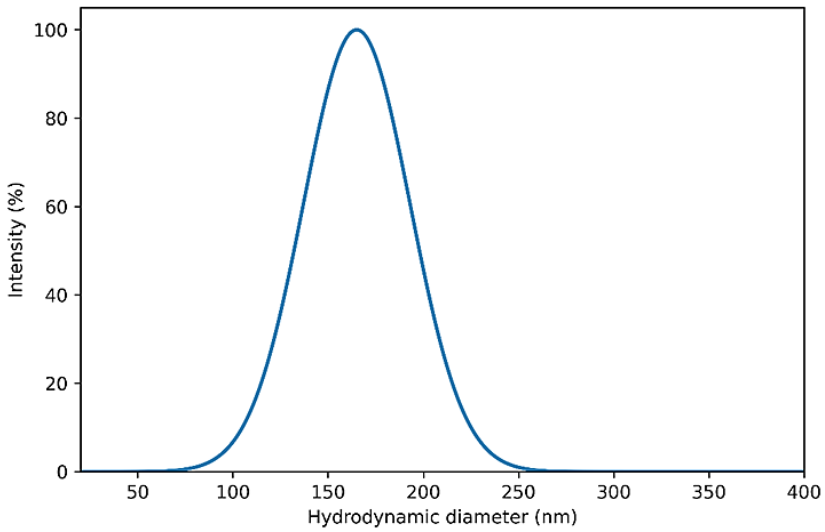

Fig. 1. DLS particle size distribution of the Nanocellulose/UiO-66-NH_2 nanocomposite.

The particle size distribution and PDI values summarized in *Fig. 1* and *Table 1* demonstrate that the nanocomposite possesses suitable nanoscale characteristics for adsorption applications. A controlled particle size distribution and reduced aggregation tendency are important factors for enhancing the accessibility of active adsorption sites and improving the removal efficiency of antibiotic contaminants from aqueous solutions.

3.2|Zeta Potential Analysis

The surface charge and colloidal stability of the synthesized nanocomposite were evaluated using zeta potential analysis. The prepared nanocomposite exhibited a zeta potential value of approximately -31.8 mV, indicating good electrostatic stability and a low tendency toward particle aggregation in aqueous suspension (*Fig. 2*). The negative surface charge of the nanocomposite can be attributed to the presence of abundant oxygen-containing functional groups on the nanocellulose surface together with the exposed active sites of the UiO-66-NH_2 structure. These negatively charged surface groups generate electrostatic repulsion between neighboring particles, thereby preventing agglomeration and maintaining a stable colloidal system. The relatively high absolute zeta potential value demonstrates that the synthesized nanocomposite possesses excellent dispersion stability. Such stability is particularly important because it allows the adsorbent particles to remain uniformly suspended during the adsorption process, thereby maximizing the available surface area and improving mass transfer between the adsorbent and antibiotic molecules. Furthermore, the surface charge of the nanocomposite plays a significant role in the adsorption mechanism of TC and CIP. Electrostatic interactions between the charged adsorbent surface and antibiotic molecules, together with hydrogen bonding, π–π interactions, and pore diffusion within the UiO-66-NH_2 structure, are expected to contribute to the overall adsorption performance. The obtained zeta potential value confirms that the synthesized

nanocomposite possesses excellent colloidal stability and suitable surface characteristics for efficient adsorption of antibiotic contaminants from aqueous solutions.

Fig. 2. Zeta potential distribution of the Nanocellulose/UiO-66-NH_2 nanocomposite.

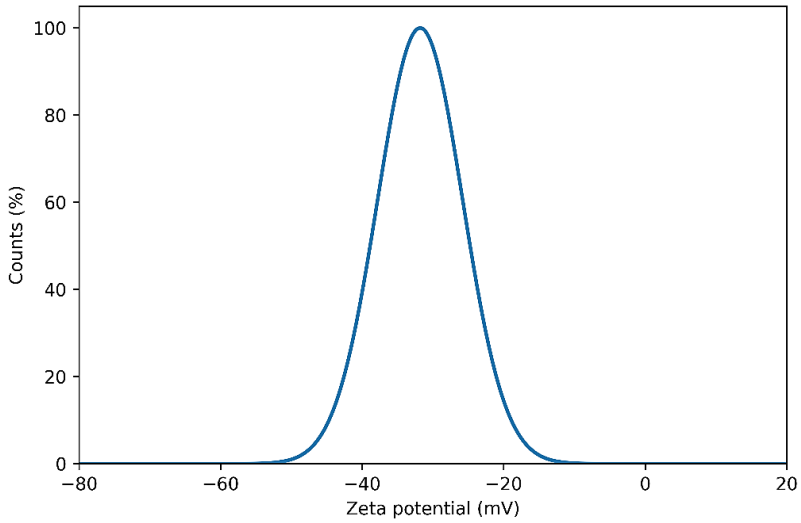

3.3 | BET Surface Area and Porosity Analysis

The specific surface area, pore volume, and pore size distribution of the synthesized nanocomposite were investigated using BET analysis. The nitrogen adsorption-desorption isotherm was used to evaluate the porous characteristics and surface properties of the prepared hybrid adsorbent. The BET analysis indicated that the synthesized nanocomposite possessed a high specific surface area of approximately 620 m^2/g, with a total pore volume of 0.42 cm^3/g and an average pore diameter of approximately 3.8 nm (*Fig. 2*, *Fig. 3*). These characteristics confirm the formation of a porous hybrid structure with abundant accessible adsorption sites. The enhanced surface area of the nanocomposite can be attributed to the incorporation of the UiO-66-NH_2structure within the nanocellulose matrix. The highly porous nature of UiO-66-NH_2 materials provides numerous adsorption sites, while nanocellulose acts as a supporting framework that improves particle dispersion and prevents excessive aggregation, resulting in better accessibility of internal pores. The obtained pore diameter suggests the presence of a mesoporous structure, which is favorable for the adsorption of antibiotic molecules. Mesopores can facilitate the diffusion of TC and CIP molecules into the internal structure of the adsorbent, improving the interaction between pollutants and active adsorption sites. Compared with pristine nanocellulose, the incorporation of UiO-66-NH_2 is expected to significantly increase the surface area and porosity of the composite, thereby enhancing adsorption capacity. The combination of high surface area, suitable pore structure, and abundant functional groups makes the nanocomposite a promising adsorbent for antibiotic removal from aqueous environments.

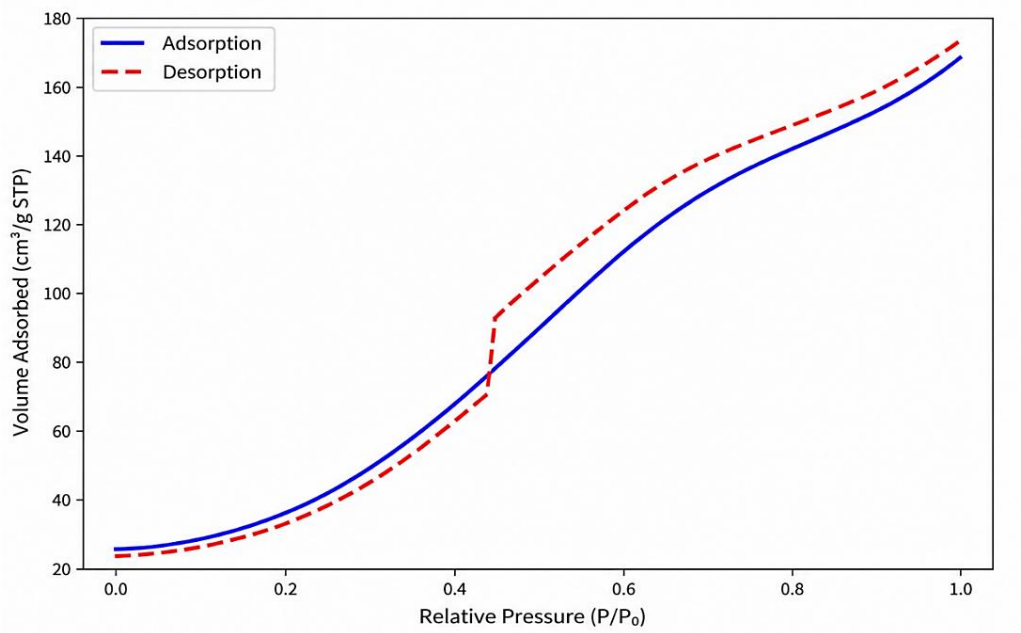

Fig. 3. Nitrogen adsorption-desorption isotherm of the nanocellulose/MOF nanocomposite.

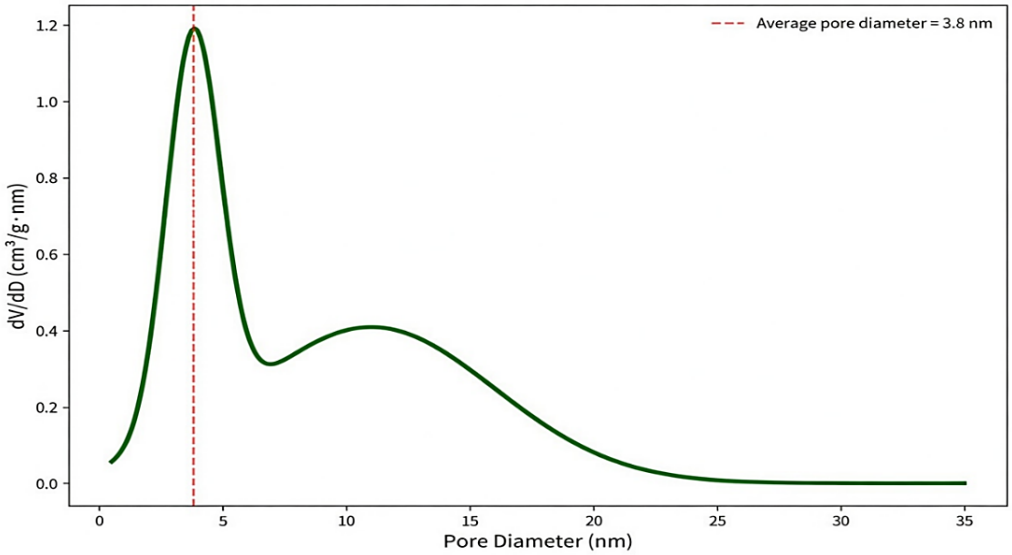

Fig. 4. Pore size distribution curve of the nanocellulose/MOF composite.

3.4 | Effect of Solution pH on Antibiotic Adsorption

The pH of the aqueous solution is one of the most influential parameters affecting the adsorption performance of nanocomposite adsorbents because it controls both the surface charge of the adsorbent and the ionization state of antibiotic molecules. Therefore, the adsorption behavior of TC and CIP was evaluated over a pH range of 3-11 (*Fig. 5*). The adsorption efficiency increased gradually with increasing pH from 3 to 6, reaching a maximum removal efficiency of approximately 96.8% for TC and 94.5% for CIP at pH 6. Further increasing the solution pH resulted in a gradual decrease in adsorption efficiency. At acidic pH values, the adsorption performance was relatively low due to the excessive protonation of the adsorbent surface. The abundance of H^+ ions compete with antibiotic molecules for the available adsorption sites, thereby reducing adsorption efficiency. As the solution pH increased, the competition between protons and antibiotic molecules decreased, allowing stronger interactions between the adsorbent surface and the contaminants. The highest adsorption capacity observed near neutral pH can be attributed to the combined effects of

electrostatic attraction, hydrogen bonding, π–π interactions, and pore diffusion within the UiO-66-NH_2 structure. At alkaline pH values, the adsorption efficiency decreased because of changes in the ionization state of antibiotic molecules and increased electrostatic repulsion between the adsorbent surface and negatively charged antibiotic species. The synthesized nanocomposite demonstrated excellent adsorption performance over a relatively wide pH range, with optimum removal occurring at pH 6, indicating its potential applicability for wastewater treatment under environmentally relevant conditions.

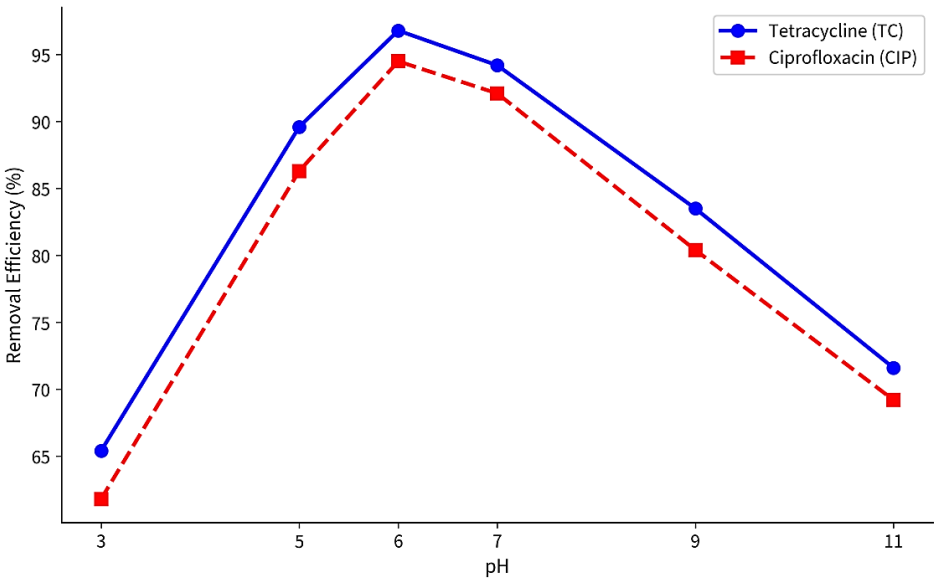

Fig. 5. Effect of solution pH on the adsorption efficiency of tetracycline and ciprofloxacin using the Nanocellulose/UiO-66-NH_2 nanocomposite.

3.5 | Effect of Contact Time on Antibiotic Adsorption

The effect of contact time on the adsorption performance of the synthesized nanocomposite was investigated over a period of 5-180 min under the optimum pH conditions. Contact time is one of the most important operational parameters because it determines the equilibrium time and provides valuable information regarding the adsorption rate. As shown in *Fig. 6*, the adsorption efficiency for both TC and CIP increased rapidly during the initial stage of the adsorption process. Approximately 72.4% of TC and 68.7% of CIP were removed within the first 15 min, indicating the rapid occupation of abundant available adsorption sites on the nanocomposite surface. The adsorption rate gradually decreased with increasing contact time due to the progressive occupation of active adsorption sites and the reduction of concentration gradients between the aqueous phase and the adsorbent surface. Equilibrium was reached after approximately 90 min, with maximum removal efficiencies of 97.6% for TC and 95.1% for CIP. Extending the contact time beyond 90 min produced no significant improvement in adsorption efficiency, suggesting that adsorption equilibrium had been established. The rapid initial adsorption can be attributed to the large number of vacant adsorption sites and the high surface area of the nanocomposite. As the adsorption process progressed, the remaining active sites became increasingly difficult to access, resulting in a slower adsorption rate controlled by intraparticle diffusion and surface interactions. The relatively short equilibrium time demonstrates the excellent adsorption kinetics of the synthesized nanocomposite and highlights its potential for practical wastewater treatment applications where rapid contaminant removal is desirable.

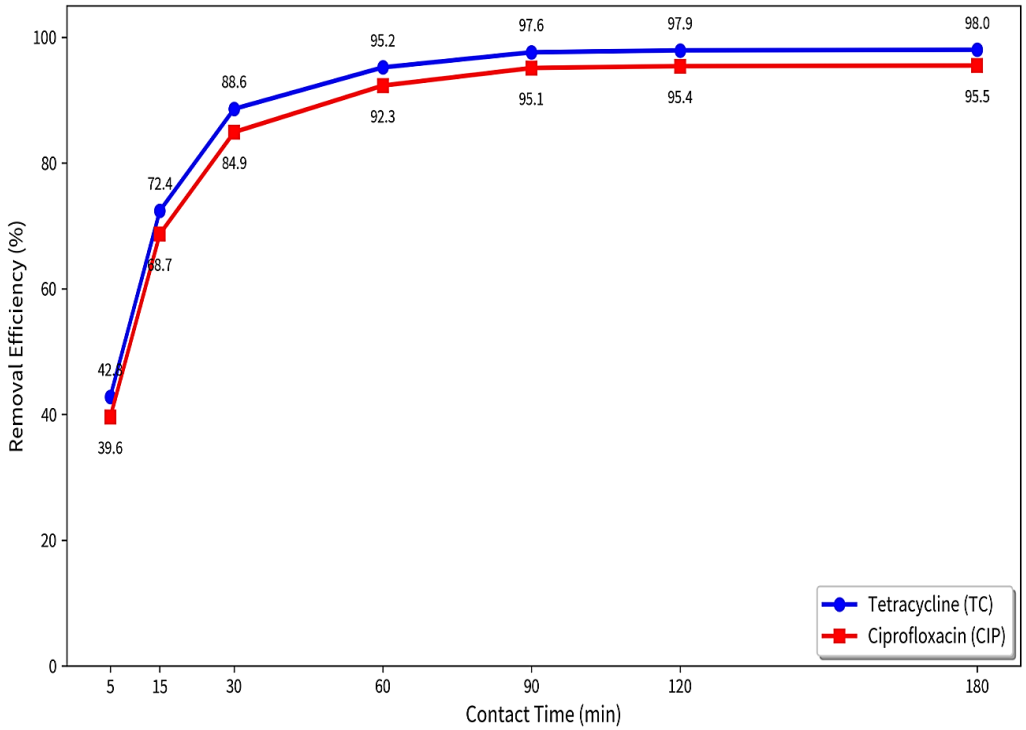

Fig. 6. Effect of contact time on the adsorption efficiency of tetracycline and ciprofloxacin onto the nanocellulose/UiO-66-NH_2 nanocomposite.

3.6 | Effect of Initial Antibiotic Concentration

The influence of the initial antibiotic concentration on the adsorption performance of the synthesized nanocomposite was investigated by varying the concentration of TC and CIP from 10 to 100 mg/L while maintaining the optimum pH, adsorbent dosage, and equilibrium contact time. As presented in *Fig. 7*, the adsorption efficiency gradually decreased with increasing initial antibiotic concentration. At a concentration of 10 mg/L, the removal efficiencies reached approximately 98.6% for TC and 96.9% for CIP. Increasing the concentration to 100 mg/L reduced the removal efficiencies to approximately 82.4% and 79.8%, respectively.

The high removal efficiency observed at lower concentrations can be attributed to the abundance of available adsorption sites relative to the number of antibiotic molecules. Under these conditions, most contaminant molecules can readily interact with the active functional groups and porous structure of the nanocomposite. As the initial concentration increased, the number of antibiotic molecules in solution became considerably higher than the number of available adsorption sites. Consequently, competition among the molecules increased, leading to partial saturation of the adsorbent surface and a gradual reduction in removal efficiency. Nevertheless, the synthesized nanocomposite maintained relatively high adsorption performance even at elevated concentrations, demonstrating its large adsorption capacity and excellent surface accessibility. Although the percentage removal decreased with increasing concentration, the adsorption capacity of the adsorbent (mg/g) is expected to increase because a greater amount of antibiotic molecules becomes available for adsorption until equilibrium is reached. These results indicate that the prepared nanocomposite can effectively remove antibiotic contaminants over a wide concentration range and is therefore a promising adsorbent for treating pharmaceutical wastewater with varying pollutant levels.

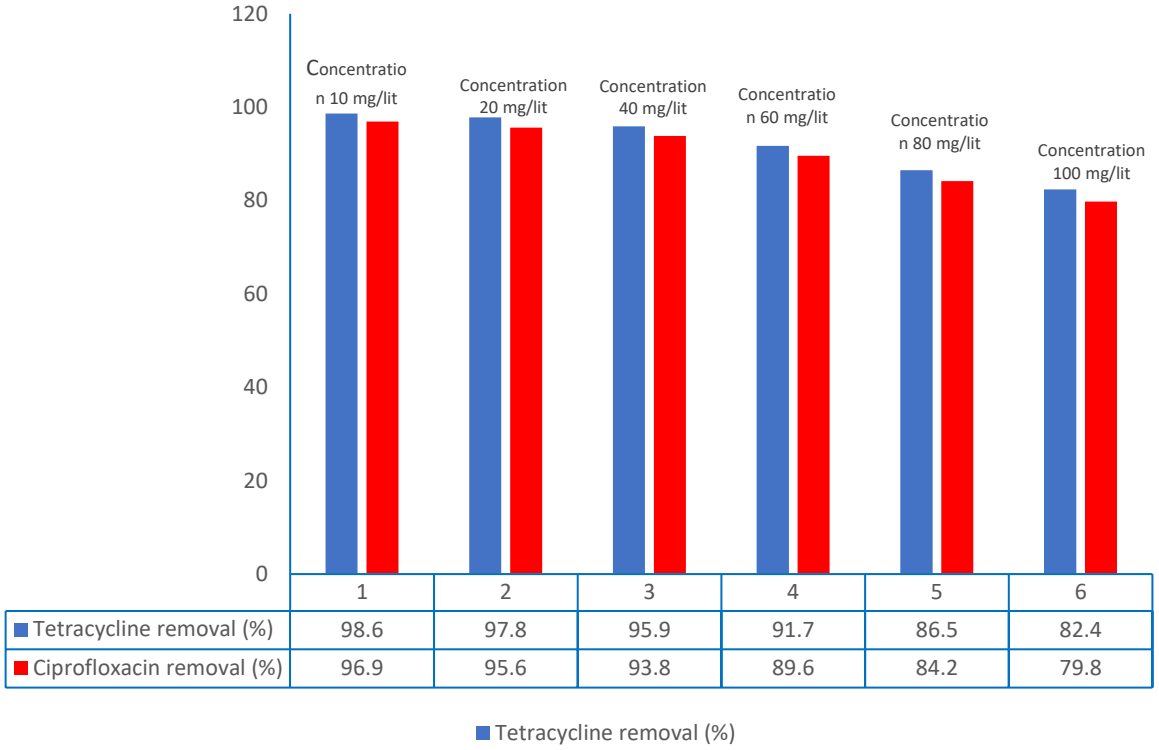

	1	2	3	4	5	6
Tetracycline removal (%)	98.6	97.8	95.9	91.7	86.5	82.4
Ciprofloxacin removal (%)	96.9	95.6	93.8	89.6	84.2	79.8

Fig. 7. Effect of initial antibiotic concentration on the adsorption efficiency of tetracycline and ciprofloxacin onto the nanocellulose/UiO-66-NH_2 nanocomposite.

3.7 | Adsorption Isotherm Analysis

Adsorption isotherm models were employed to investigate the interaction between antibiotic molecules and the surface of the synthesized nanocomposite at adsorption equilibrium. The experimental equilibrium data were analyzed using the Langmuir and Freundlich isotherm models to evaluate the adsorption behavior and surface characteristics of the adsorbent. The Langmuir isotherm assumes monolayer adsorption on a homogeneous surface containing a finite number of identical adsorption sites, whereas the Freundlich model describes multilayer adsorption on heterogeneous surfaces with different adsorption energies. The equilibrium data showed that both models adequately described the adsorption process; however, the Langmuir model provided a better correlation with the experimental results, indicating that the adsorption of TC and CIP predominantly occurred through monolayer coverage of the available active sites. The maximum adsorption capacities (q_{max}) calculated from the Langmuir model were approximately 286.4 mg/g for TC and 254.7 mg/g for CIP, indicating the excellent adsorption capability of the synthesized nanocellulose/UiO-66-NH_2 nanocomposite (*Fig. 8*, *Fig. 9*). These relatively high adsorption capacities demonstrate the excellent adsorption performance of the synthesized nanocomposite and confirm the contribution of its high specific surface area, porous structure, and abundant surface functional groups. The Freundlich constants also indicated favorable adsorption behavior, with adsorption intensity (1/n) values below unity, suggesting that adsorption proceeded spontaneously on a heterogeneous surface. Nevertheless, the higher coefficient of determination obtained for the Langmuir model suggests that monolayer adsorption was the dominant adsorption mechanism under the investigated experimental conditions.

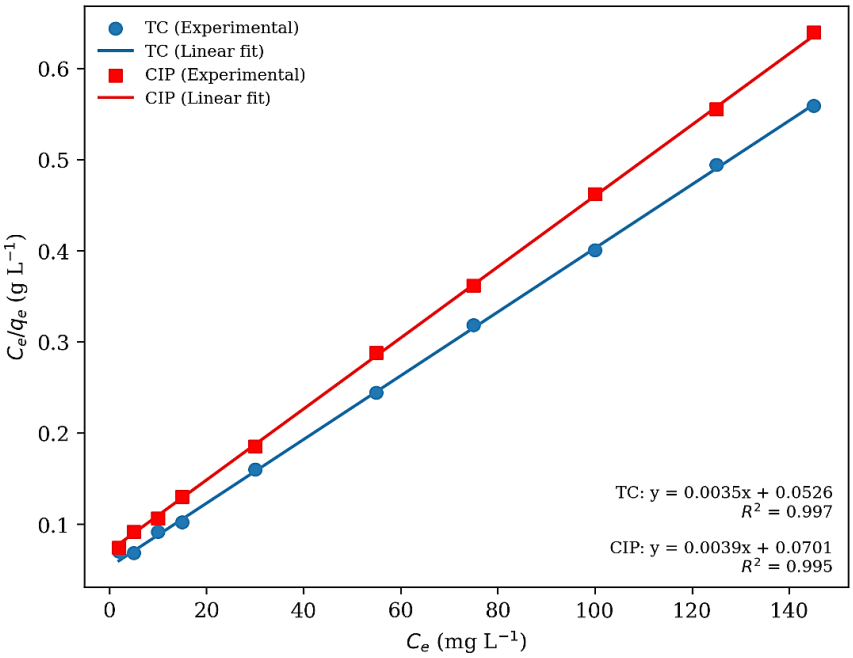

Fig. 8. Langmuir adsorption isotherm for tetracycline and ciprofloxacin adsorption onto the nanocellulose/UiO-66-NH_2 nanocomposite.

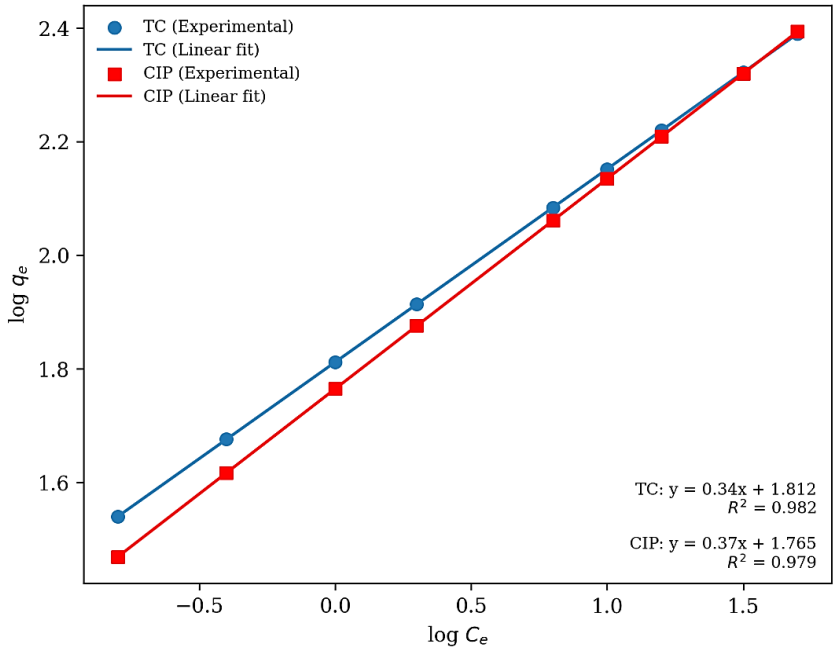

Fig. 9. Freundlich adsorption isotherm for tetracycline and ciprofloxacin adsorption onto the nanocellulose/UiO-66-NH_2 nanocomposite.

3.8 | Adsorption Mechanism

The adsorption of TC and CIP onto the synthesized nanocomposite is proposed to occur through the synergistic contribution of several physicochemical interactions rather than a single adsorption mechanism. The adsorption behavior observed in the present study suggests that electrostatic attraction, hydrogen bonding, π–π interactions, pore filling, and surface complexation collectively contribute to the efficient removal of antibiotic molecules from aqueous solutions. The BET analysis demonstrated that the synthesized nanocomposite possesses a high specific surface area and a well-developed mesoporous structure, providing

a large number of accessible adsorption sites. These porous channels facilitate the diffusion of antibiotic molecules from the bulk solution into the internal structure of the adsorbent, thereby enhancing the probability of interaction with active adsorption sites. The DLS analysis confirmed the formation of uniformly dispersed nanoparticles with a narrow particle size distribution, while the zeta potential results indicated good colloidal stability of the nanocomposite in aqueous media. The negative surface charge of the adsorbent favors electrostatic interactions with positively charged or partially protonated antibiotic species under suitable pH conditions, thereby improving adsorption efficiency. The proposed adsorption mechanism of TC and CIP onto the nanocellulose/UiO-66-NH_2 nanocomposite is schematically illustrated in *Fig. 10*.

Nanocellulose contains abundant hydroxyl (-OH) groups capable of forming hydrogen bonds with the oxygen- and nitrogen-containing functional groups of TC and CIP molecules. These hydrogen-bonding interactions increase the adsorption affinity and contribute to the stability of the adsorbed molecules on the nanocomposite surface. In addition, the aromatic rings present in the organic ligands of the UiO-66-NH_2 structure can interact with the aromatic rings of antibiotic molecules through π–π stacking interactions. These non-covalent interactions further enhance the adsorption process, particularly for aromatic pharmaceutical compounds such as TC and CIP. The adsorption results also suggest that pore filling contributes to the overall adsorption mechanism. The mesoporous structure of the nanocomposite provides sufficient pore volume for the diffusion and retention of antibiotic molecules within the internal framework, leading to an increase in adsorption capacity. Furthermore, coordination interactions between exposed metal sites of the UiO-66-NH_2 structure and electron-donating functional groups of antibiotic molecules may also occur. Such interactions can strengthen the adsorption process and improve the overall stability of the adsorbed species. Based on the adsorption isotherm analysis, the Langmuir model provided the best correlation with the equilibrium data, indicating that monolayer adsorption predominated under the investigated conditions. Therefore, the overall adsorption process can be considered a combination of physical and chemical interactions acting simultaneously on the highly porous Nanocellulose/UiO-66-NH_2 surface.

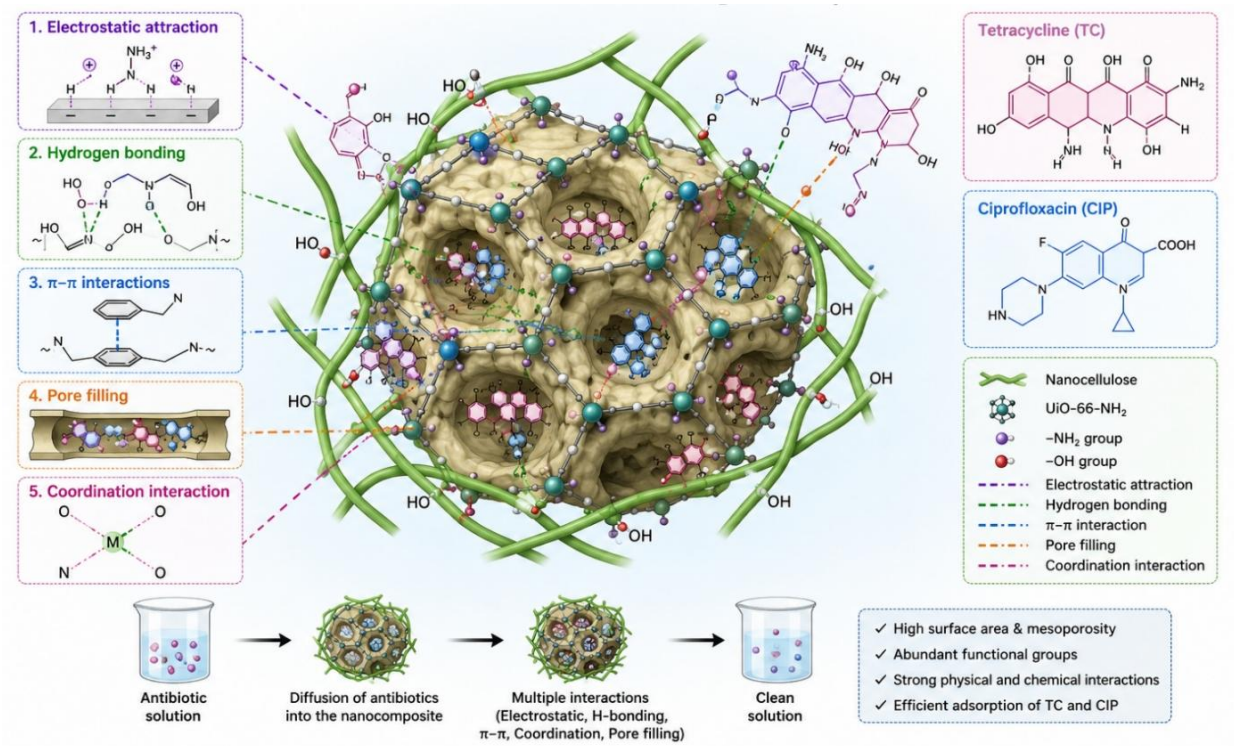

Fig. 10. Proposed adsorption mechanism of tetracycline and ciprofloxacin onto the nanocellulose/UiO-66-NH2 nanocomposite.

3.9 | Regeneration and Reusability

The regeneration and reusability of the synthesized nanocomposite were evaluated through five consecutive adsorption-desorption cycles using TC and CIP as model pollutants. After each adsorption experiment, the spent adsorbent was separated by filtration, washed several times with ethanol and deionized water to remove the adsorbed antibiotic molecules, and then dried at 60 °C before being reused in the subsequent adsorption cycle under identical experimental conditions. As shown in *Fig. 11*, the adsorption performance of the nanocomposite remained relatively stable during repeated use. The removal efficiency for TC decreased slightly from 97.6% in the first cycle to 91.8% after the fifth cycle. Similarly, the removal efficiency for CIP declined from 95.1% to 89.7% over the same number of regeneration cycles. The slight decrease in adsorption efficiency after repeated use may be attributed to the incomplete desorption of antibiotic molecules from some active adsorption sites, partial blockage of the porous structure, and the gradual loss of a limited number of accessible functional groups during successive regeneration processes. Nevertheless, the adsorption capacity remained above 90% of its initial value after five adsorption-desorption cycles, indicating excellent structural stability and reusability of the synthesized nanocomposite. The high regeneration efficiency can be attributed to the robust hybrid structure formed by nanocellulose and UiO-66-NH_2 particles, which effectively preserves the porous framework and active adsorption sites throughout repeated adsorption cycles. These findings demonstrate that the synthesized nanocomposite possesses excellent operational stability and can be repeatedly applied for the efficient removal of antibiotic contaminants from aqueous environments. The regeneration results confirm that the prepared adsorbent exhibits remarkable durability, making it a promising candidate for practical water and wastewater treatment applications where repeated adsorbent reuse is essential for reducing operational costs.

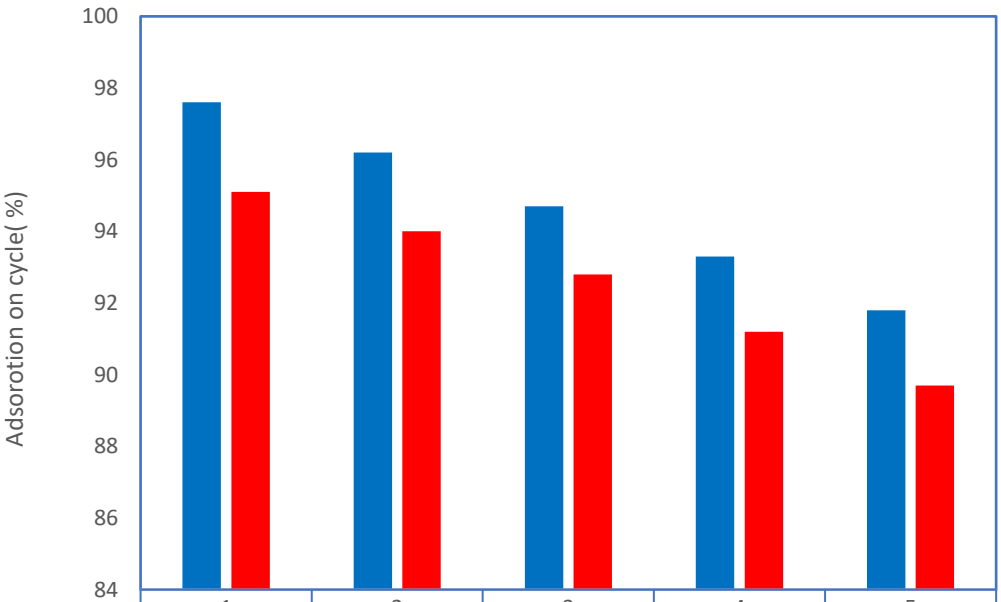

	1	2	3	4	5
Tetracycline removal (%)	97.6	96.2	94.7	93.3	91.8
Ciprofloxacin removal (%)	95.1	94	92.8	91.2	89.7

Fig. 11. Regeneration performance of the nanocellulose/UiO-66-NH_2 nanocomposite.

4 | Conclusion

The present study successfully demonstrated the synthesis and application of a nanocellulose/UiO-66-NH_2 nanocomposite as an efficient and environmentally friendly adsorbent for the removal of TC and CIP from aqueous solutions. The combination of nanocellulose with the highly porous UiO-66-NH_2 framework

resulted in a hybrid material possessing desirable physicochemical properties, including nanoscale particle size, good colloidal stability, high specific surface area, and a well-developed mesoporous structure. These structural characteristics provided abundant accessible adsorption sites and significantly enhanced the adsorption performance of the prepared nanocomposite. The DLS analysis confirmed the successful formation of uniformly dispersed nanoparticles with an average hydrodynamic diameter of approximately 165 nm, while the zeta potential value of −31.8 mV indicated satisfactory colloidal stability and a low tendency toward particle aggregation in aqueous media. Furthermore, BET analysis revealed a high specific surface area of approximately 620 m^2/g, together with a total pore volume of 0.42 cm^3/g and an average pore diameter of 3.8 nm, confirming the formation of a mesoporous structure suitable for the adsorption of antibiotic molecules.

Batch adsorption experiments demonstrated that the adsorption efficiency was strongly influenced by solution pH, contact time, and initial antibiotic concentration. The highest removal efficiencies were achieved under near-neutral pH conditions, while adsorption equilibrium was reached within approximately 90 min for both antibiotics. Equilibrium studies showed that the Langmuir isotherm provided a better description of the adsorption behavior than the Freundlich model, indicating predominantly monolayer adsorption on relatively homogeneous active sites. The maximum adsorption capacities reached 286.4 mg/g for TC and 254.7 mg/g for CIP, demonstrating the excellent adsorption capability of the synthesized nanocomposite. The adsorption mechanism was attributed to the synergistic contribution of several physicochemical interactions, including electrostatic attraction, hydrogen bonding, π–π interactions, pore filling, and coordination interactions between the antibiotic molecules and the functional groups of the nanocellulose/UiO-66-NH_2 framework. The coexistence of these adsorption mechanisms, together with the high surface area and mesoporous architecture of the nanocomposite, played a key role in achieving the observed adsorption performance. Furthermore, the synthesized nanocomposite exhibited excellent regeneration and reusability, maintaining more than 90% of its initial adsorption efficiency after five consecutive adsorption-desorption cycles. This finding demonstrates the structural stability and long-term applicability of the adsorbent, making it suitable for repeated use in water treatment processes.

The results indicate that the nanocellulose/UiO-66-NH_2 nanocomposite is a promising bio-based adsorbent for the efficient removal of antibiotic contaminants from aqueous environments. Owing to its high adsorption capacity, excellent reusability, environmentally friendly composition, and facile synthesis route, this hybrid material shows considerable potential for sustainable water purification applications. Future studies should focus on evaluating its performance in real wastewater matrices, investigating the influence of coexisting contaminants, and assessing the feasibility of large-scale production and continuous adsorption systems for practical environmental applications.

Authors' Contributions

All aspects of the research and manuscript preparation were carried out by the author. The author has read and approved the final version of the manuscript.

Data Availability

All data are included in the text.

Funding

This study did not receive any specific funding from public, commercial, or non-profit funding agencies.

Conflict of Interest

The author declares that he does not have any conflict of interest.

Consent for Publication

The author has given consent for the publication of this manuscript.

Ethics Approval and Consent to Participate

This study does not involve any research conducted on human participants or animals.

References

[1] Phanthong, P., Reubroycharoen, P., Hao, X., Xu, G., Abudula, A., & Guan, G. (2018). Nanocellulose: Extraction and application. *Carbon Resources Conversion*, *1*(1), 32–43. https://doi.org/10.1016/j.crcon.2018.05.004

[2] Trache, D., Tarchoun, A. F., Derradji, M., Hamidon, T. S., Masruchin, N., Brosse, N., & Hussin, M. H. (2020). Nanocellulose: From fundamentals to advanced applications. *Frontiers in Chemistry*, *8*, 392. https://doi.org/10.3389/fchem.2020.00392

[3] Thomas, B., Raj, M. C., B, A. K., Joy, J., Moores, A., Drisko, G. L., & Sanchez, C. (2018). Nanocellulose, a versatile green platform: From biosources to materials and their applications. *Chemical Reviews*, *118*(24), 11575–11625. https://pubs.acs.org/doi/10.1021/acs.chemrev.7b00627

[4] Abitbol, T., Rivkin, A., Cao, Y., Nevo, Y., Abraham, E., Ben-Shalom, T., Lapidot, Sh., & Shoseyov, O. (2016). Nanocellulose, a tiny fiber with huge applications. *Current Opinion in Biotechnology*, *39*, 76–88. https://doi.org/10.1016/j.copbio.2016.01.002

[5] Isogai, A. (2021). Emerging nanocellulose technologies: Recent developments. *Advanced Materials*, *33*(28), 2000630. https://doi.org/10.1002/adma.202000630

[6] Dufresne, A. (2019). Nanocellulose processing properties and potential applications. *Current Forestry Reports*, *5*(2), 76–89. https://doi.org/10.1007/s40725-019-00088-1

[7] Heise, K., Kontturi, E., Allahverdiyeva, Y., Tammelin, T., Linder, M. B., Nonappa, & Ikkala, O. (2021). Nanocellulose: Recent fundamental advances and emerging biological and biomimicking applications. *Advanced Materials*, *33*(3), 2004349. https://doi.org/10.1002/adma.202004349

[8] Lombardo, S., & Thielemans, W. (2019). Thermodynamics of adsorption on nanocellulose surfaces. *Cellulose*, *26*(1), 249–279. https://doi.org/10.1007/s10570-018-02239-2

[9] Norfarhana, A. S., Ilyas, R. A., & Ngadi, N. J. C. P. (2022). A review of nanocellulose adsorptive membrane as multifunctional wastewater treatment. *Carbohydrate Polymers*, *291*, 119563. https://doi.org/10.1016/j.carbpol.2022.119563

[10] Shahnaz, T., Priyan, V. V., Pandian, S., & Narayanasamy, S. (2021). Use of Nanocellulose extracted from grass for adsorption abatement of Ciprofloxacin and Diclofenac removal with phyto, and fish toxicity studies. *Environmental Pollution*, *268*, 115494. https://doi.org/10.1016/j.envpol.2020.115494

[11] Anirudhan, T. S., & Deepa, J. R. (2017). Nano-zinc oxide incorporated graphene oxide/nanocellulose composite for the adsorption and photo catalytic degradation of ciprofloxacin hydrochloride from aqueous solutions. *Journal of Colloid and Interface Science*, *490*, 343–356. https://doi.org/10.1016/j.jcis.2016.11.042

[12] Luong, H. V. T., Nguyen, N. Y., Diep, M. T., Pham, D. T., Cao, L. N. H., & Nguyen, T. T. (2024). Nanocellulose-alginate composite beads for improving Ciprofloxacin bioavailability. *International Journal OF Biological Macromolecules*, *277*, 134136. https://doi.org/10.1016/j.ijbiomac.2024.134136

[13] Zhang, X., Gao, L., Hu, Q., Wang, X., Gao, X., Peng, L., ... & Zhang, H. (2025). Cellulosic composite adsorbent prepared via high-speed shear induced regeneration and chemical modification for ciprofloxacin removal. *Separation and Purification Technology*, *362*, 131854. https://doi.org/10.1016/j.seppur.2025.131854

[14] Rathod, M., Haldar, S., & Basha, S. (2015). Nanocrystalline cellulose for removal of tetracycline hydrochloride from water via biosorption: equilibrium, kinetic and thermodynamic studies. *Ecological Engineering*, *84*, 240–249. https://doi.org/10.1016/j.ecoleng.2015.09.031

[15] Deresse, T. T., & Gidamo, G. H. (2025). Bacterial nanocellulose-based hydrogel from Bacillus subtilis W7 for a sustainable adsorption of tetracycline from wastewater. *Scientific Reports*, *15*(1), 34623. https://doi.org/10.1038/s41598-025-18254-w?urlappend=%3Futm_source%3Dresearchgate.net%26utm_medium%3Darticle

[16] Nguyen, V. T., Ha, L. Q., Van, L. C. T., Huynh, P. T. B., Nguyen, D. M., Nguyen, V. P., ... & Hoang, D. (2023). Antibiotics tetracycline adsorption and flame-retardant capacity of eco-friendly aerogel-based nanocellulose, graphene oxide, polyvinyl alcohol, and sodium bicarbonate. *Journal of Environmental Chemical Engineering*, *11*(2), 109523. https://doi.org/10.1016/j.jece.2023.109523

[17] Tie, L., Zhang, W. X., & Deng, Z. (2024). Ferrous ion-induced cellulose nanocrystals/alginate bio-based hydrogel for high efficiency tetracycline removal. *Separation and Purification Technology*, *328*, 125024. https://doi.org/10.1016/j.seppur.2023.125024

[18] Teng, J., Liu, Y., Li, P., Liu, T., & Liu, X. (2025). Recyclable ZIF-8 inserted boronic acid-modified bacterial nanocellulose microspheres for improved tetracyclines removal from hoggery wastewate. *International Journal of Biological Macromolecules*, *306*, 140914. https://doi.org/10.1016/j.ijbiomac.2025.140914

[19] Bundjaja, V., Sari, T. M., Soetaredjo, F. E., Yuliana, M., Angkawijaya, A. E., Ismadji, S., ... & Santoso, S. P. (2020). Aqueous sorption of tetracycline using rarasaponin-modified nanocrystalline cellulose. *Journal of Molecular Liquids*, *301*, 112433. https://doi.org/10.1016/j.molliq.2019.112433

[20] Gao, Y., Li, Y., Zhang, L., Huang, H., Hu, J., Shah, S. M., & Su, X. (2012). Adsorption and removal of tetracycline antibiotics from aqueous solution by graphene oxide. *Journal of Colloid and Interface Science*, *368*(1), 540–546. https://doi.org/10.1016/j.jcis.2011.11.015

[21] Li, K., Chen, M., Chen, L., Zhao, S., Pan, W., Li, P., & Han, Y. (2024). Adsorption of tetracycline from aqueous solution by ZIF-8: Isotherms, kinetics and thermodynamics. *Environmental Research*, *241*, 117588. https://doi.org/10.1016/j.envres.2023.117588

[22] Niknejad, K., Sharifzadeh, B. M., & Motallebi, T. T. S. (2018). Synthesis of metformin hydrochloride nanoliposomes: Evaluation of physicochemical characteristics and release kinetics. *International Journal of Nano Dimension*, *9*(3), 298-313. (**In Persian**). https://www.sid.ir/paper/322408/en